NASA/TP—2004–213143

Plasma Sail Concept Fundamentals

G.V. Khazanov
Marshall Space Flight Center, Marshall Space Flight Center, Alabama

P. Delamere
University of Colorado, Boulder, Colorado

K. Kabin
University of Alberta, Edmonton, Canada

T.J. Linde
The University of Chicago, Chicago, Illinois

April 2004

The NASA STI Program Office…in Profile

Since its founding, NASA has been dedicated to the advancement of aeronautics and space science. The NASA Scientific and Technical Information (STI) Program Office plays a key part in helping NASA maintain this important role.

The NASA STI Program Office is operated by Langley Research Center, the lead center for NASA's scientific and technical information. The NASA STI Program Office provides access to the NASA STI Database, the largest collection of aeronautical and space science STI in the world. The Program Office is also NASA's institutional mechanism for disseminating the results of its research and development activities. These results are published by NASA in the NASA STI Report Series, which includes the following report types:

- TECHNICAL PUBLICATION. Reports of completed research or a major significant phase of research that present the results of NASA programs and include extensive data or theoretical analysis. Includes compilations of significant scientific and technical data and information deemed to be of continuing reference value. NASA's counterpart of peer-reviewed formal professional papers but has less stringent limitations on manuscript length and extent of graphic presentations.

- TECHNICAL MEMORANDUM. Scientific and technical findings that are preliminary or of specialized interest, e.g., quick release reports, working papers, and bibliographies that contain minimal annotation. Does not contain extensive analysis.

- CONTRACTOR REPORT. Scientific and technical findings by NASA-sponsored contractors and grantees.

- CONFERENCE PUBLICATION. Collected papers from scientific and technical conferences, symposia, seminars, or other meetings sponsored or cosponsored by NASA.

- SPECIAL PUBLICATION. Scientific, technical, or historical information from NASA programs, projects, and mission, often concerned with subjects having substantial public interest.

- TECHNICAL TRANSLATION. English-language translations of foreign scientific and technical material pertinent to NASA's mission.

Specialized services that complement the STI Program Office's diverse offerings include creating custom thesauri, building customized databases, organizing and publishing research results…even providing videos.

For more information about the NASA STI Program Office, see the following:

- Access the NASA STI Program Home Page at http://www.sti.nasa.gov

- E-mail your question via the Internet to help@sti.nasa.gov

- Fax your question to the NASA Access Help Desk at (301) 621–0134

- Telephone the NASA Access Help Desk at (301) 621–0390

- Write to:
  NASA Access Help Desk
  NASA Center for AeroSpace Information
  7121 Standard Drive
  Hanover, MD 21076–1320
  (301)621–0390

Plasma Sail Concept Fundamentals

G.V. Khazanov
Marshall Space Flight Center, Marshall Space Flight Center, Alabama

P. Delamere
University of Colorado, Boulder, Colorado

K. Kabin
University of Alberta, Edmonton, Canada

T.J. Linde
The University of Chicago, Chicago, Illinois

Acknowledgments

Available from:

TABLE OF CONTENTS

LIST OF FIGURES

LIST OF ACRONYMS

AMPTE	Active Magnetospheric Particle Trace Explorers
CRRES	Combined Release and Radiation Effects Satellite
M2P2	mini-magnetospheric plasma propulsion
MHD	magnetohydrodynamic
TP	Technical Publication

NOMENCLATURE

$\mathbf{B}$	magnetic field
B_1	variable field
$\mathbf{B}_{dp}$	curl free dipole field
$\mathbf{B}_0$	ambient curl free interplanetary magnetic field
B_y	component of the interplanetary magnetic field
c	speed of light
$\mathbf{E}$	electric field
e	electronic charge
$\mathbf{F}$	aerodynamic force
I	unit tensor
$\mathbf{J}$	plasma current density
k	Boltzmann's constant
L	length scale
L_B	magnetic field length scale
L_n	plasma density length scale
m_e	electron mass
m_i	ion mass
N	dimensionless ratio
n	density
n_d	dust density
n_f	fluid density
n_p	particle density
n_{SW}	solar wind density
P	momentum
P_c	momentum of the plasma cloud/obstacle
p	pressure

R	radial coordinate
R_c	radius of the cloud
r	radial coordinate
r_d	grain size
S	surface area
T_d	plasma temperature
T_e	electron temperature
T_{ij}	stress tensor
t	time
$\mathbf{u}$	plasma bulk flow velocity
$\mathbf{u}_e$	electron flow velocity
$\mathbf{u}_f$	fluid flow velocity
$\mathbf{u}_p$	particle velocity
$\mathbf{v}$	velocity
v	plasma velocity
V	velocity
v_A	local Alfvén velocity of the ambient plasma
v_C	cloud velocity
v_n	component of velocity normal to the control volume surface
v_{SW}	solar wind velocity
x	horizontal axis
y	vertical axis
ε	energy density
θ	magnetic latitude
ρ	mass density
τ	time scale
δ_{ij}	unit tensor
μ_0	magnetic permeability of free space
ω_{pi}	ion plasma frequency

TECHNICAL PUBLICATION

PLASMA SAIL CONCEPT FUNDAMENTALS

1. INTRODUCTION

The mini-magnetospheric plasma propulsion (M2P2) device, originally proposed by Winglee et al.,[1] predicts that a 15-km standoff distance (or 20-km cross-sectional dimension) of the magnetic bubble will provide for sufficient momentum transfer from the solar wind to accelerate a spacecraft to unprecedented speeds of 50–80 km/s after an acceleration period of ≈3 mo. Such velocities will enable travel out of the solar system in a period of ≈7 yr—almost an order of magnitude improvement over present chemical-based propulsion systems. The plasma sail produces thrust for the spacecraft by absorbing momentum from the hypersonic solar wind. Coupling to the solar wind is accomplished through a magnetic bubble created by injecting plasma into a magnetic field generated by solenoid coils located on the spacecraft. The plasma sail is a new and very promising propulsion mechanism, but it invokes specific and complex physical processes that must be studied carefully.

Winglee et al.[1] used a multifluid plasma model which treats solar wind and injected ions as well as electrons as separate species. Their estimation of the size of the magnetic bubble was based on extrapolation of the results obtained from several simulations of systems much smaller than M2P2. This Technical Publication (TP) shows, however, that in the case of Winglee et al.,[1] a fluid model has no validity for such a small-scale size—even in the region near the plasma source. It is assumed in the MHD model, normally applied to planetary magnetospheres, that the characteristic scale size is much greater than the Larmor radius and ion skin depth of the solar wind. In the case of M2P2, however, the size of the magnetic bubble is actually less than or comparable to the scale of these characteristic parameters. Therefore, a kinetic approach which addresses the small-scale physical mechanisms must be used.

To the authors' knowledge, there are currently only two preliminary attempts to use a kinetic approach to model an M2P2 system.[2,3] Both of these efforts are based on a hybrid plasma model. The study by Saha et al.[2] was focused on the formation of a magnetic bubble, studying the $1/r$ magnetic field dependence predicted by Winglee et al.[1] However, their work could not verify the predicted size of M2P2. Karimabadi and Omidi,[3] assuming the $1/r$ magnetic field dependence as given, investigated momentum transfer from the solar wind to a magnetic bubble. They found that the degree of ion reflection needed for momentum transfer, 20 to 50 percent, is approached only when the standoff distance is ≈0.7 times the ion skin depth of the impinging solar wind (≈100 km). This is much larger than in the size of the M2P2 device described by Winglee et al.[1] Karimabadi and Omidi[3] conclude that the results by Winglee et al.[1] should be reconsidered using the kinetic simulations. It should be noted, however, that their conclusion is based on a two-dimensional model in which they used a prescribed magnetic field dependence of $1/r$ and they neglected plasma inside the magnetic bubble.

Preliminary experimental studies showed only some very simple qualitative features of the M2P2 magnetic field configuration created by expanding internal plasma and its interaction with streaming external plasma.[4] The authors submit, however, it is not possible to achieve an exact scaling of the total M2P2-solar wind interaction in the laboratory. Therefore, while these experiments provided a very qualitative picture of a magnetic bubble, because of the scaling limitations, they do not provide a useful description of the formation and characteristics of a plasma-inflated bubble required for a full-scale plasma sail.

The goal of this TP is, therefore, a focused and systematic investigation that is designed to elucidate the basic physical processes involved in plasma sail formation. Specifically, based on the main characteristics of the current state of knowledge of plasma sails, the investigation will be focused on the following three fundamental questions:

(1) What approach should be used to describe a plasma sail formation?

(2) What is the spatial dependence of the plasma sail's magnetic field?

(3) What is the total force generated on the plasma sail by solar fluxes?

These issues are described in detail in sections 2 and 3. Each issue is crucial to the question of plasma sail feasibility and can be clearly identified for study by the combined magnetohydrodynamic (MHD) and kinetic theoretical approach.

2. APPROACH

The physical scale lengths associated with the plasma sail problem vary from centimeters to hundreds of kilometers. This is why the different approaches must be used to verify each physical principle that will be addressed in this TP. Each method, based on MHD transport equations or a kinetic description, has advantages and disadvantages. Therefore, they should not be regarded as mutually exclusive or competing approaches, but rather as complementary techniques that should all contribute to understanding plasma sail operation in space. To demonstrate this, new combined MHD and kinetic studies of the plasma sail propulsion concept are presented.

2.1 Magnetohydrodynamic Studies

The efficiency of the M2P2 plasma sails' propulsion critically depends on the fact that the magnetic field in the plasma bubble changes as $1/r$ starting from the coil on the spacecraft. This dependence of the magnetic field was suggested by Winglee et al.[1] based on a series of MHD simulations with the parameters significantly different from the proposed plasma sail configuration. In their simulations, Winglee et al.[1] gradually increased the magnetic field and associated plasma injection at an inner boundary of 10 m until it reached a magnetic field strength of 4,000 nT. Such a magnetic field strength and injection speed of 20 km/s lead to an ion Larmor radius of ≈50 m and make fluid simulations inapplicable even in the region near the injection boundary. The $1/r$ dependence of the magnetic field was also used by Winglee et al.[1] to extrapolate the magnetic field from their inner simulation boundary of 10 m to the coil size of 10 cm. This procedure leads to the estimation that a 1kG (0.1T) magnetic field at the coil will result in an effective plasma sail. Thus, in view of the above concerns, the conclusions reached by Winglee et al.[1] regarding the M2P2 system size and the required magnetic field strength on the spacecraft must be verified. Therefore, the M2P2 calculations have been carried out using more comprehensive theoretical tools.

The multiscale adaptive MHD model that is being used in the studies incorporates some of the most important recent advances in the numerical methods for MHD and is briefly described in appendix A. This MHD model has been successfully applied to a variety of space plasma processes and structures, such as the comet—solar wind interaction, magnetospheres of planets and satellites, and heliosphere.[5–8] For Saturnian satellite Titan, the results obtained with the single-fluid MHD model were compared with the results of a multifluid model.[9] As discussed by Nagy et al.,[9] the multifluid description provides relatively insignificant changes to the overall structure of the Titan-Saturnian magnetospheric interaction, which lends credibility to the plasma sail studies presented in this TP.

To ensure the applicability of the MHD approach in the plasma source region, this model was run with the magnetic field at the inner boundary ($R=10$ m) fixed at $6×10^5$ nT. This is the value suggested by Winglee et al.[1] as sufficient for the plasma sail to capture enough of the solar wind momentum to be a practical concept. This estimation for the required magnetic field intensity was obtained by Winglee et al.[1] as an extrapolation of their simulations with much weaker fields; e.g., 4,000 nT at the 10-m inner boundary. In the simulation the solar wind density, velocity, and temperature were chosen to be 6 cm^{-3}, 500 km/s, and 10 eV, respectively. The interplanetary magnetic field was set to 10 nT purely in the

y direction. These parameters are fairly representative of the conditions of Earth's orbit and are similar to those used by Winglee et al.[1] At the 10-m boundary, a plasma density of 1.7×10^{10} amu/cm^3, a spherical plasma outflow velocity of 20 km/s, and a plasma temperature of 5 eV were specified. The magnetic field was set to a pure dipole with an equatorial strength of 6×10^5 nT at 10 m. All of these parameters were selected to correspond to the suggestions of Winglee et al.[1] for an operational plasma sail configuration.

The full-sized M2P2 modeling results are shown in figures 1 and 2. Figure 1 shows the density structure (a) on the global scale and (b) near the region of the source. In this figure, one can see a bow shock at *r*≈80 km in the subsolar direction. Behind this discontinuity the supersonic solar wind starts to divert around the obstacle presented by the plasma sail. At *r*=40 km there is a magnetopause which in this simulation is a discontinuity separating solar wind ions from the injected ions. This simulated result indicates a much bigger size of the mini-magnetosphere as compared to work by Winglee et al.[1] This difference can most likely be attributed to the fact that a spherically symmetric plasma outflow at 10 m was assumed. In contrast, Winglee et al.[1] did not use symmetric loading. Other possible sources of the discrepancy may be associated with the uncertainty of the Winglee et al.[1] extrapolation and the slightly different MHD formalism assumed in the two models.

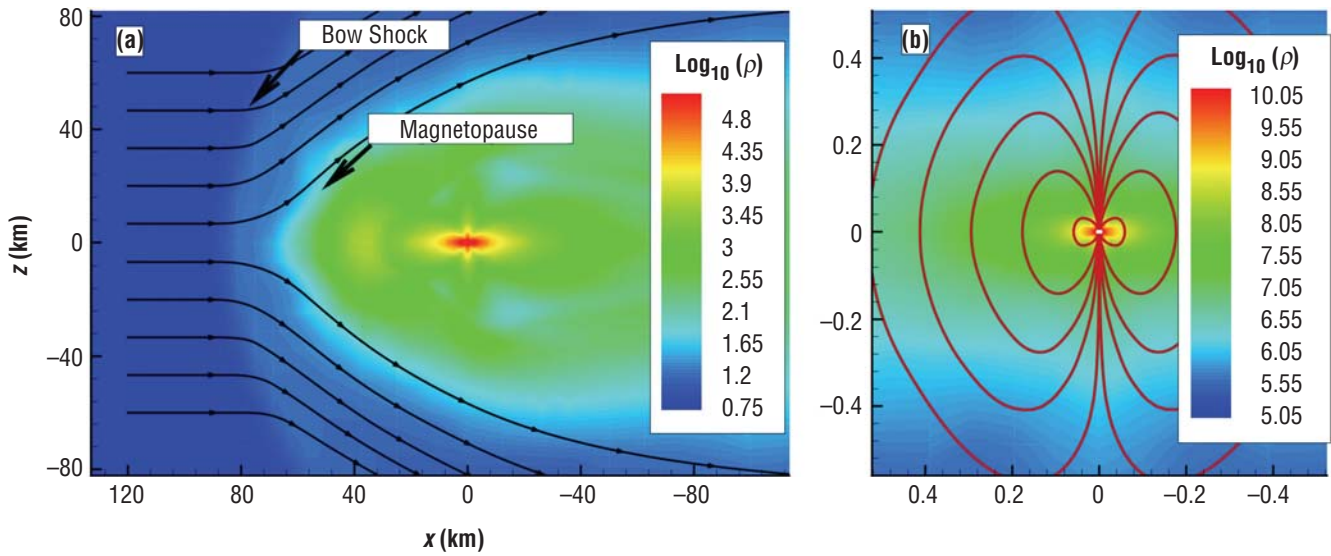Figure 1. The density structure from an MHD simulation (a) on a global scale and (b) near the region of the source. Density is in units of amu/cm^3. Black lines in (a) are the solar wind flow lines which are seen to divert around the magnetopause; locations of the bow shock and magnetopause are indicated. Red lines in (b) are the magnetic field lines.

Figure 2 presents the magnetic field magnitude falloff in the subsolar direction. In this plot the magnetopause appears as a sharp increase in the magnetic field intensity at 40 km as the magnetic barrier forms in the shocked solar wind plasma to counteract the expanding ejected plasma. This is the region of the most intense currents outside the spacecraft. Magnetic forces acting between these currents and those in the coil onboard the spacecraft are ultimately responsible for the momentum transfer between the solar

wind and the plasma sail device. The bow shock in figure 2 is seen at ≈80 km where the magnetosheath magnetic field drops to the magnetic field value in the solar wind. The black line in figure 2 shows the magnetic field behavior in a simulation without the solar wind; i.e., a simulation in which the injected plasma expands into an empty space. It is seen that up to ≈25 km the plasma expansion is unaffected by the solar wind. The distance at which the solar wind effects become noticeable obviously depends on the solar wind conditions. The blue line in figure 2 shows the results of a similar simulation in which the solar wind dynamic pressure was increased by a factor of 3. Not surprisingly, in the simulation with the higher solar wind dynamic pressure, both the bow shock and the magnetopause are pushed closer to the spacecraft. Also, as shown in figure 2, the magnetic field has more complicated behavior than that predicted by Winglee et al.[1] Specifically, near the region of the plasma source the magnetic field intensity falls off as $1/r^2$ and not $1/r$ as it was predicted by Winglee et al.[1] Therefore, both the magnetic field strength at the spacecraft and the electric power required to produce it are somewhat underestimated in the work of Winglee et al.[1]
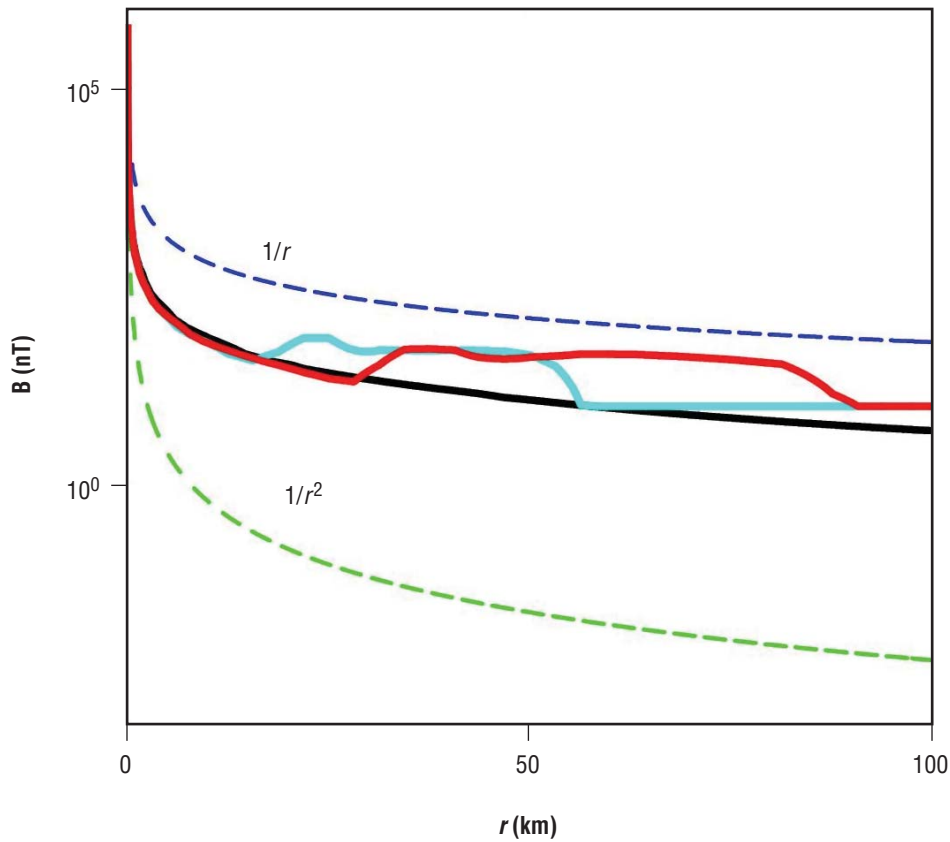

Figure 2. The magnetic field falloff in the subsolar direction. The red line indicates MHD simulation with solar wind, the black line indicates MHD simulation without solar wind, and the blue line indicates MHD simulation with solar wind with increased dynamic pressure; thin dashed lines show $1/r$ and $1/r^2$ dependencies for comparison.

5

The MHD results presented above lead to a very important conclusion regarding the stepwise approach that can be used in the theoretical studies of plasma sail phenomena. This approach justifies separation of the plasma source-controlled and solar wind-controlled regions of the magnetic bubble, which can greatly simplify the theoretical studies of plasma sails. Specifically, the results from the source-controlled region can be used as the boundary conditions for kinetic simulations that must be carried out in the solar wind-controlled region of the magnetic bubble.

To ensure a smooth interface and the validity of these MHD and kinetic results, the selection of the lower boundary for the kinetic studies must be justified. The first desire is to take this boundary at the distance of 25 km, where there is still a source-controlled region, in order to avoid large variations in scales of plasma sails and greatly simplify the numerical implementation of the kinetic code. It was not the case in this study. The following criteria to be satisfied were selected in order to pick this distance as far as possible from the spacecraft: (1) The characteristic scale size at this boundary is much greater than the Larmor radius and ion skin depth of the source and (2) the MHD solution of source-controlled region must be valid. The first criterion is very obvious and easy to check based on the parameter values predicted by the MHD solution presented in section 1. The second criterion required some additional scale analysis in order to check applicability of the hydromagnetic approximation used in the MHD studies versus the generalized Ohm's law. Such analysis can be performed based on the approach developed by Siscoe.[10] The idea of such analysis is to compare the $\mathbf{v} \times \mathbf{B}$ term in the generalized Ohm's law with all other terms and make it comfortably larger than all of them. Such comparison leads to the following dimensionless ratios that have only been slightly modified in order to reflect the nature of the plasma sail problem:

$$N_1 = \frac{\mu_0 e^2}{m_e} nVL_B\tau; \quad N_2 = \frac{e}{k}\frac{VBL_n}{T_e}; \quad N_3 = e\mu_0\frac{nVL_B}{B}; \quad N_4 = \frac{\mu_0 e^2}{m_e}nL_B^2 \; . \tag{1}$$

In these expressions, L_B and L_n represent the characteristic length of the magnetic field and plasma density defined as

$$L_B = \left|\frac{B}{\partial B / \partial \vec{r}}\right| \text{ and } L_n = \left|\frac{n}{\partial n / \partial \vec{r}}\right| , \tag{2}$$

and are calculated based on MHD solutions; τ is the time between the electron and ion collisions. Figure 3 shows the calculation of N_{1-4} dimensionless ratios between 1 and 25 km. Combining these calculations with the calculations of the Larmor radius and ion skin depth of the source particles, one can comfortably place the low boundary for the kinetic simulations at a distance of 5 km from the spacecraft.

It should be noted that uniform injection of the plasma in the radial direction in a dipolar magnetic field creates toroidal electric field, which causes a continuous addition of the magnetic flux to the plasma bubble. The steady state is achieved when the rate at which the magnetic flux is added to the system equals the rate at which it is removed by reconnection at the magnetopause. To investigate the importance of this additional magnetic flux on the system, a separate MHD simulation in which plasma was injected parallel to the magnetic field lines at the inner boundary was performed. In this case $\mathbf{v} \times \mathbf{B} = 0$ and no magnetic flux is added to the plasma bubble. The plasma injection speed was chosen to be proportional to $\cos^2(\theta)$, where θ is the magnetic latitude. Thus, the injection speed varied from 20 km/s at the magnetic pole where the field lines are radial to zero at the magnetic equator where the field lines are perpendicular to the radial

direction. The results of this simulation are qualitatively very similar to the previous results. The size of the plasma bubble is somewhat smaller than before with the bow shock located at 50 km instead of 80 km. However, in this case the rate of plasma loss is also smaller than in the case of spherically symmetric injection. It should be emphasized that the MHD approximation is not valid over the length scales of the plasma sail; hence, all of the results of section 2.1 are only preliminary estimations.
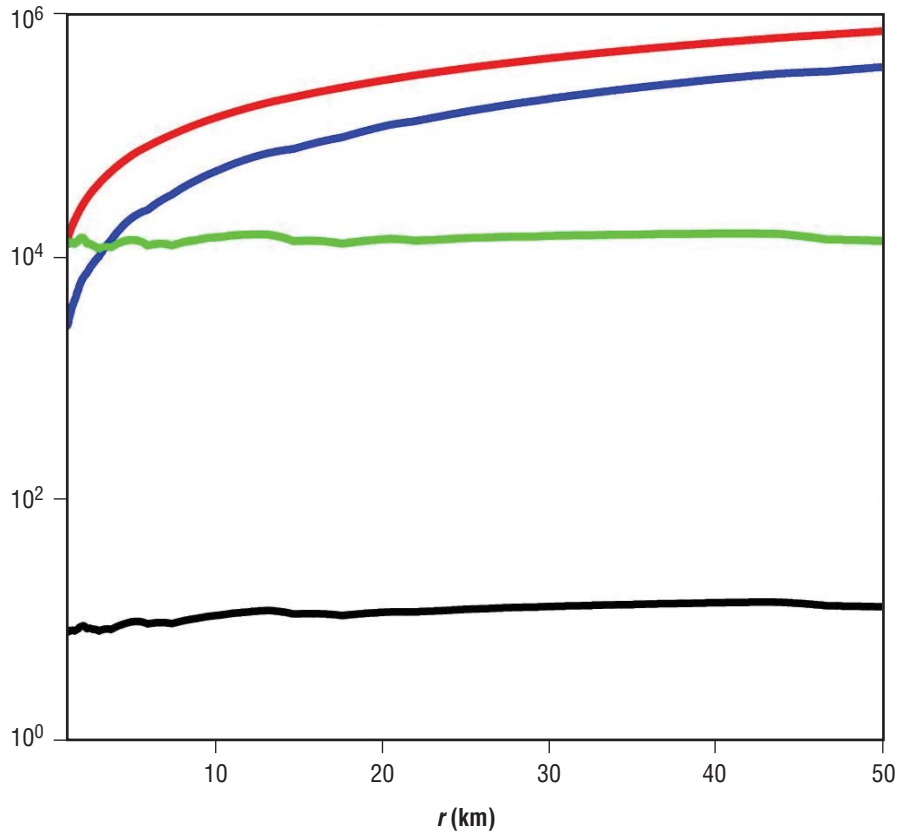

Figure 3. Dimensionless ratios between 1 and 25 km based on an MHD simulation. N_1 is shown by the red line, N_2 by the blue line, N_3 by the black line, and N_4 by the green line.

2.2 Kinetic Studies

The ion Larmor radius (hundreds of kilometers) and ion inertial length ($\approx$70 km) of the solar wind protons are greater than or comparable to the size of the magnetic bubble predicted by MHD studies. It is, therefore, questionable if any of the fluid approaches should be used in describing the momentum transfer from the solar wind to the system. Ion kinetic effects are important in a number of naturally occurring plasma systems in space plasmas. Obvious examples include the solar wind interaction with small solar system objects such as comets, planetary satellites, and small planets, such as Mars or Pluto. Other situations where ion kinetic effects are important include boundary regions in space. The M2P2 plasma sail system represents a similar class of problem. A critical issue facing the plasma sail concept is the role of ion kinetic effects in coupling solar wind energy and momentum to the spacecraft. While the

dense inner regions of the magnetic bubble may be well suited to a fluid description where the ions are strongly magnetized, the outer region of the bubble is dominated by ion kinetic effects.

Perhaps the closest relatives to a plasma sail are the many active plasma experiments that have been conducted in Earth's space environment over the past three decades. For example, a fully three-dimensional version of the hybrid code that is used in these plasma sail studies was originally developed by Delamere et al.[11,12] for the plasma injection experiments made as a part of the Combined Release and Radiation Effects Satellite (CRRES) mission. The mathematical formalism and numerical details of this model are described in these papers and briefly outlined in appendix B. This code is used here in the combined MHD and kinetic code.

The hybrid code provides a kinetic description for the ions and a fluid description for the electrons. A kinetic description is not necessary for the dense inner regions of the magnetic bubble and tremendous computational savings can be realized by treating this dense, magnetized ion population with the fluid description. The hybrid simulation used the steady-state output from the MHD model interpolated to a 5-km resolution grid to specify the initial magnetic field configuration over a 5×5×5 subarray centered on the source grid. The total magnetic field was then described by contributions from the fixed solar wind and MHD input magnetic fields and the perturbation magnetic fields calculated self consistently by the hybrid code. Particles were injected from the center of the source grid into the magnetic bubble with an average injection velocity of 20 km/s such that the density in the source grid cell was maintained at the steady-state MHD value for the 5-km surface. The solar wind particles were initialized with a directed velocity of 500 km/s and randomized thermal component of 1 eV. A minimum of 10 solar wind particles per cell was maintained in the simulation. The upstream inflow boundary preserved the upstream solar wind density while the downstream outflow boundary allowed particles to exit the simulation domain. All other boundaries were periodic. The simulation was run for one solar wind transit time across the simulation domain (105×45×37 grid cells).

Figure 4 shows in red the position of all source particles projected onto the *x-y* plane. Figure 4(a) is the case of kinetic treatment of the solar wind and source particles; figure 4(b) is the case of cold fluid treatment of the solar wind and kinetic treatment of the source population. The solar wind ion density contours are calculated for an initial density of 10 cm^{-3}. In the kinetic case (fig. 4(a)), the solar wind particles form two density enhancements in the downstream regions and the source particles are lost from the bubble in the transverse direction. In the fluid case (fig. 4(b)), the source particles are lost predominantly in the downstream direction due to the uniform force exerted by the MHD modes throughout the source region. In the pure MHD case shown in figure 1, the plasma sail is highly symmetric.

Significant density structures developed in the wake region for the kinetic case. Two density enhancements are seen downstream as "prongs." The plasma losses from the magnetic bubble also show significant differences. In figure 4(a) the particles are lost transverse to the solar wind flow, while in figure 4(b) the particles are lost primarily in the downstream direction. In the case of a purely kinetic treatment of all ion particles (fig. 4(a)), no upstream bow shock formed and no heating of the solar wind protons occurred throughout the interaction region. The implications of these differences between fluid and kinetic treatments are discussed in the context of momentum transfer in section 3.
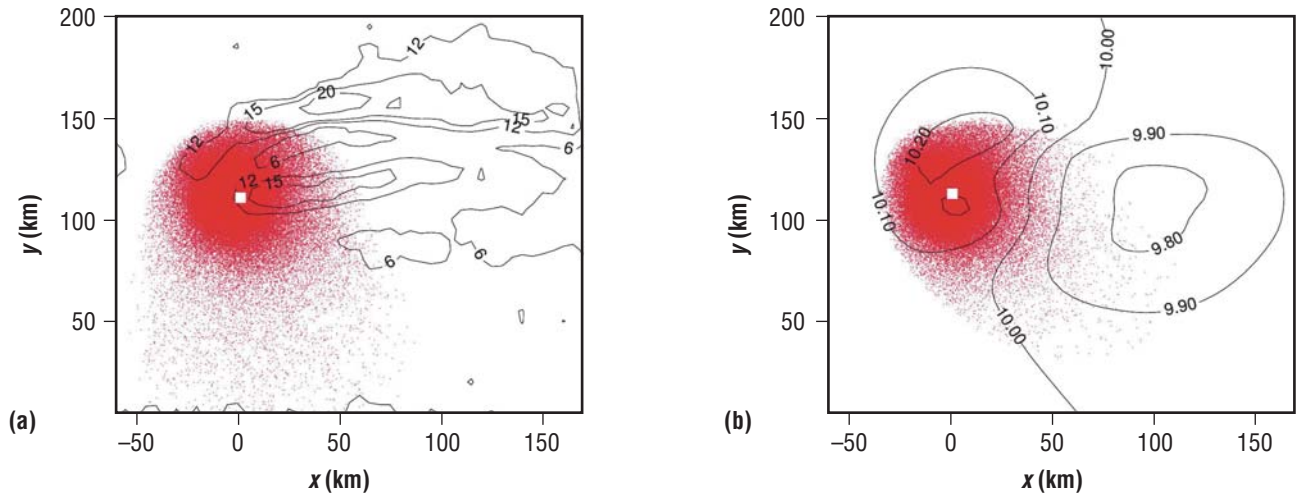
Figure 4. Comparison of (a) kinetic and (b) fluid treatment of the solar wind in the plasma sail interaction; the contours show the density of the solar wind particles and the source particles are indicated in red.

Figure 5 illustrates the current systems from the hybrid simulation in the downstream wake region in the plane perpendicular to the solar wind flow. The topology of the current system is similar to the current systems found in the Earth's magnetotail and is also similar to the current systems described by Winglee et al.[1] that couple momentum from the solar wind to the magnetic bubble. However, as discussed in section 3, the momentum transfer in the kinetic treatment is very different from that of both the MHD and two-fluid treatments.
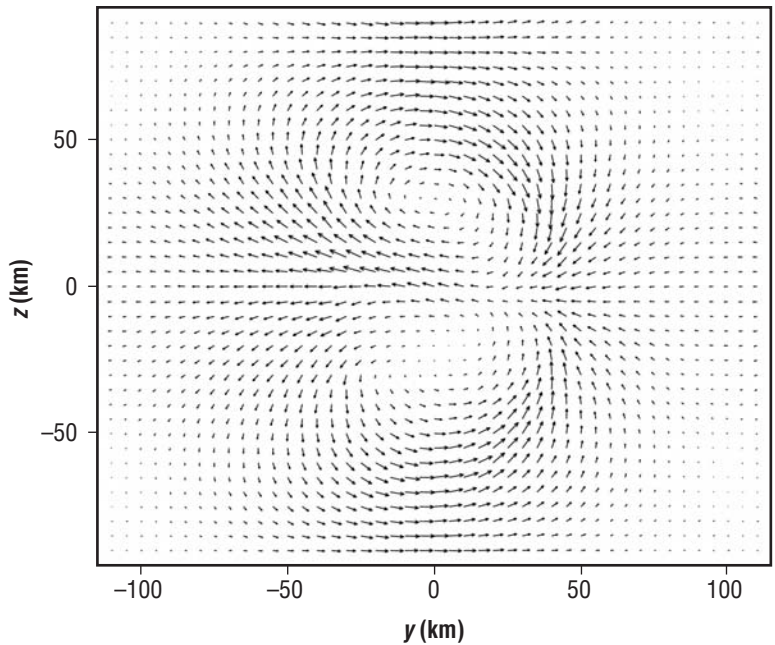

Firgure 5. Currents from the hybrid simulation in the downstream region perpendicular to the solar wind flow direction.

3. MOMENTUM TRANSFER

The kinetic model of the interaction between the solar wind and plasma sail illustrates the fundamental importance of ion kinetic effects in transferring momentum from the solar wind to the plasma sail. The plasma sail represents a physical system where the length scales, L, are considerably smaller than the upstream ion inertial length. A similar interaction occurs in the case of small, magnetized asteroids. Wang and Kivelson[13] demonstrated that the asteroid/solar wind interaction is mediated by whistler waves rather than MHD modes; i.e., compressional modes and shear Alfvén waves, when the length scale of the interaction volume is smaller than the upstream ion inertial length (c/ω_{pi}). A comparison of model results with magnetometer data from the Galileo spacecraft confirmed the whistler-mediated interaction. More recently, two-dimensional hybrid code simulations by Omidi and Karimabadi[3] showed that the transition from a whistler-mediated to an MHD-mediated interaction occurs for $L \approx 0.7 (c/\omega_{pi})$; however, this transition may take place at even larger length scales in the three-dimensional case. The nature of momentum transfer is fundamentally different for these two cases as discussed in the context of the plasma sail application.

In the MHD approximation, the solar wind interaction with the plasma sail produces several current systems most important of which are the magnetopause and bow shock currents. As described by Winglee et al.,[1] for example, these currents exert magnetic forces on the spacecraft electromagnet, thus providing a momentum transfer from the solar wind to the spacecraft. A direct calculation of these forces is, however, an extremely tedious numerical procedure requiring multiple integrations over the whole three-dimensional computational volume. Fortunately, this entire procedure can be bypassed and the momentum transfer from the solar wind flow to the plasma sail can be calculated using the momentum theorem of fluid mechanics which gives the following expression for aerodynamic force:[14]

$$\mathbf{F} = \iint_S \rho v_n \mathbf{v} dS \ , \tag{3}$$

where S is a sufficiently large control volume enclosing the central body, $\mathbf{v}$ is the gas or plasma velocity, v_n is the component of the velocity normal to the control volume surface, and ρ is the mass density.

This expression holds in MHD as well, as long as displacement currents and, therefore, momentum of the electromagnetic field are neglected. Evaluating this integral numerically, a force in the direction of the solar wind flow of ≈ 5 N is found from the MHD simulation. Although the B_y component of the interplanetary magnetic field leads to some asymmetry of the plasma flow around the plasma sail, this asymmetry does not produce any noticeable component of the force perpendicular to the undisturbed solar wind flow.

For an MHD-mediated interaction, the momentum transfer can be understood with the frozen-in condition for magnetofluids; the momentum transfer rate for a plasma cloud moving relative to a magnetized plasma is $dP_c / dt \approx -2\pi R_c^2 \rho v_A v_c$ where P_c is the momentum of the plasma cloud/obstacle, v_A is the local Alfvén velocity of the ambient plasma, v_c is the cloud velocity, ρ is the solar wind density,

and R_c is the radius of the cloud.[12] Using the model parameters for the solar wind conditions; i.e., v_{sw}=500 km/s, n_{sw}=6 cm^{-3}, the momentum transfer to the plasma sail can be estimated. Figure 1 shows that the radius of the plasma sail is roughly 40 km, so $dP_c/dt \approx 4$ N, which is in rough agreement with the MHD model calculation of 5 N. Winglee et al.[1] extrapolated their multifluid results and predicted a 20-km cross-sectional dimension and a total force of 1 N, also in agreement with the estimate. Thus, the momentum transfer mechanism, namely the Alfvénic interaction, appears to be the same for the single-fluid and multifluid approaches. Thus the MHD calculations are valid for determining momentum transfer wherever the fluid approximation is valid.

The hybrid model, however, shows that the plasma sail application cannot be understood with the frozen-in condition. For an interaction dominated by ion kinetic effects, the force on the obstacle can be understood by rewriting the $\mathbf{J} \times \mathbf{B}$ force term as $(\nabla \times \mathbf{B}) \times \mathbf{B} = (\mathbf{B} \cdot \nabla)\mathbf{B} - \nabla B^2/2$. The source region of the plasma sail experiences a force due to the draping of the magnetic field over the obstacle or tension force (first term) and a force due to magnetic pressure gradients (second term). The Alfvénic interaction generally dictates that the interaction volume will experience a uniform force due to the tension force of the draped magnetic field configuration. However, in the case of the plasma sail, the Alfvénic interaction is absent since these MHD modes cannot be excited. In this case, the currents generated by the interaction are due to the motion of pickup ions in the direction of the convection electric field ($-y$). Figure 4 illustrates the kinetic versus fluid treatments of the solar wind flow. In the kinetic treatment shown in figure 4(a), the source particles move only in the direction of the solar wind convection electric field as they do not experience a solar wind-directed magnetic tension force. In the fluid treatments shown in figure 4(b), the source particles move primarily in the solar wind direction with some lateral asymmetry due to large Larmor radius effects.

The expression for momentum conservation (app. B) for the hybrid code states that the force on the particles in a given volume element is equal to the Maxwell stresses on the surface of the volume; the electric fields do not enter this expression due to the assumption of quasi-neutrality. Figure 6 shows the force on three different volume elements centered on the source region as a function of time. The solid line shows the force on the source grid cell (5×5×5 km^3); the dotted and dashed lines show the force for progressively larger test volumes (35×35×35 km^3 and 55×55×55 km^3, respectively) containing the source cell. Note that the force on the source grid cell is nearly steady at t=0.7 s while the larger volumes experience larger forces due to the pickup of plasma lost from the magnetic bubble. The solar wind-directed force is negligible in the source region and, in fact, the force is directed upstream. Figure 7 shows contours of the total magnetic field of the magnetic bubble. The source region, the intersection of dotted lines, is offset from the peak magnetic field strength. Therefore, the source region, in the absence of an accelerating tension force, will experience forces in the lateral direction (y) and the upstream direction ($-x$) consistent with the momentum transfer calculations. For larger test volumes, the force includes the $\mathbf{J} \times \mathbf{B}$ force generated by the motion of ions picked up in the solar wind flow. A considerable lateral force is generated in the y direction consistent with the recoil of pickup ions moving in the $-y$ direction. The lateral force is analogous to the observed lateral motion of the Active Magnetospheric Particle Tracer Explorers (AMPTE) artificial comet discussed by Delamere et al.[11] Thus, careful note should be taken of the similarity between the plasma sail concept and previous active plasma experiments in space.
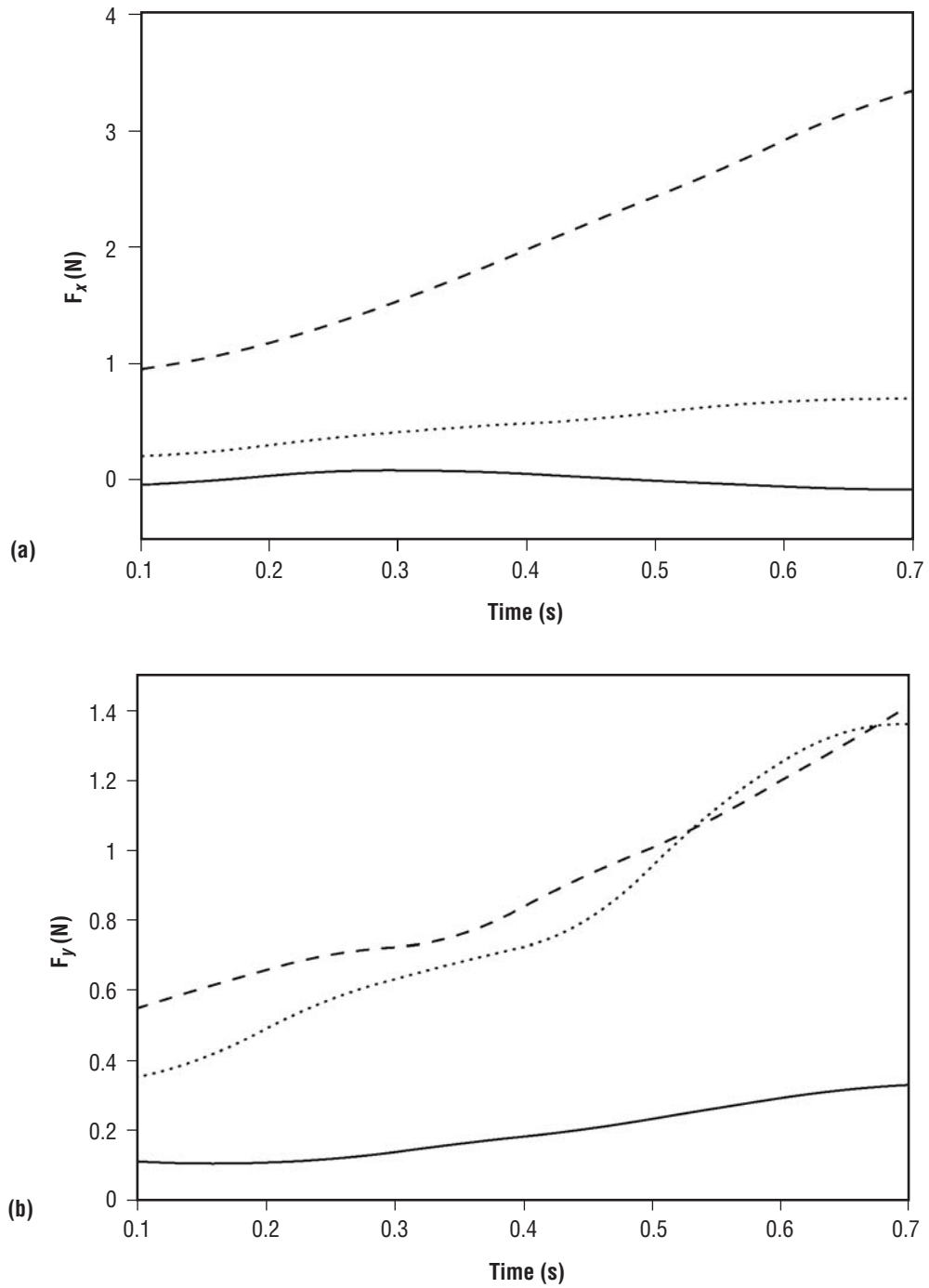
(a)

(b)

Figure 6. Momentum transfer—total force plotted as a function of time
for three different control volumes centered on the source grid
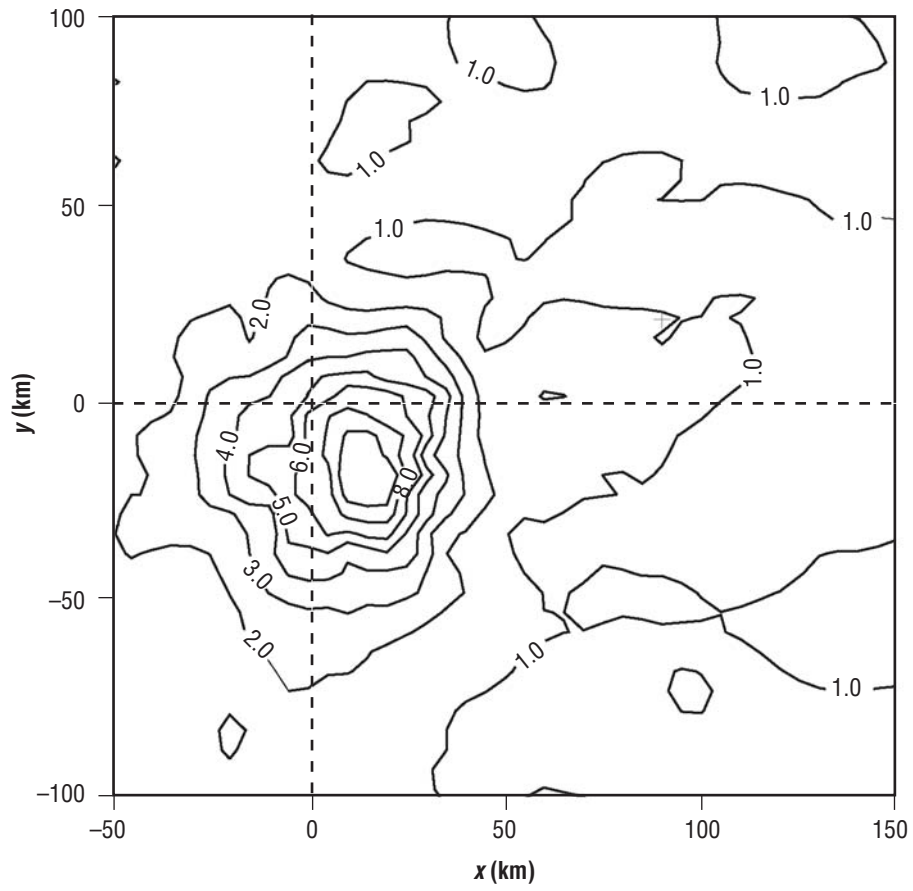in (a) the solar wind direction, x, and (b) the transverse direction, y.

13

Figure 7. Total magnetic field in the source region normalized to the interplanetary magnetic field; the source grid is located at the intersection of the dotted lines.

4. DISCUSSION AND CONCLUSION

The plasma sail produces thrust for the spacecraft by absorbing momentum from the hypersonic solar wind. Coupling to the solar wind is accomplished through a magnetic bubble created by injecting plasma into a magnetic field generated by solenoid coils located on the spacecraft. The plasma sail is a new and very promising propulsion mechanism, but it invokes specific and complex physical processes. The goal of this TP is to describe a focused and systematic investigation that is designed to elucidate the basic physical processes involved in plasma sail formation. Specifically, based on the main characteristics of the current state of knowledge of plasma sails, the investigation has been focused on the three fundamental questions summarized as follows:

(1) What approach should be used to describe a plasma sail formation? Kinetic effects strongly dictate the nature of the momentum coupling between the solar wind and the magnetic bubble. Any approach used to describe the plasma sail formation must include these effects. However, the self-consistent description of the evolution of the plasma sail is computationally intensive and considerable savings can be realized by using a fluid treatment for the innermost regions of the magnetic bubble. The fluid description is valid inside the 5-km boundary. That is, within the 5-km boundary the injected ions are strongly magnetized and the expansion of the magnetic bubble is largely independent of the solar wind conditions. Beyond 5 km, kinetic effects dictate the interaction and it is critical that a kinetic approach be adopted. A two-component approach has been implemented to describe (1) the self-consistent evolution of the magnetic bubble for realistic parameters and (2) the momentum coupling of the bubble to the solar wind. An MHD approach was used to describe the initial expansion of the bubble and the steady-state fluid conditions at the 5-km boundary were used as input for a hybrid code to determine the momentum coupling to the solar wind.

(2) What is the spatial dependence of the plasma sail's magnetic field? Self-consistent MHD studies of the expansion of the magnetic bubble show complicated behavior ranging from $1/r^2$ to constant (fig. 2). In the region near the plasma source the magnetic field falls off initially as $1/r^2$, not $1/r$ as predicted. The assumption of a $1/r$ magnetic field dropoff near the plasma source, therefore, leads to an underestimation of the magnetic field strength needed at the spacecraft and therefore the required power. The expansion of the magnetic bubble is mostly unaffected by the solar wind flow out to the 25 km subsolar point.

(3) What is the total force generated on the plasma sail by solar fluxes? Although the self-consistent hybrid/fluid approach to investigating the evolution and subsequent coupling of the plasma sail to the solar wind is still under investigation, preliminary results suggest that MHD modes cannot be excited and, hence, momentum transfer to the spacecraft may be limited. However, the possibility of capturing solar radiation as a momentum source may provide a viable alternative. A complete discussion of this issue is provided in section 4.2.

15

4.1 Plasma Sail Feasibility

The main motivation for and benefit of this study was to provide sufficient insight into the feasibility of the plasma sail concept. Using a two-component approach for modeling the self-consistent evolution of the magnetic bubble; i.e., for the configuration described by Winglee et al.[1] and the momentum coupling to the solar wind, it is concluded that the momentum transfer to the spacecraft is considerably smaller than was predicted for M2P2. For similar momentum transfer a larger plasma sail would be required for an MHD-mediated interaction. For typical solar wind conditions, the MHD modes; i.e., Alfvén mode, can only be excited when the cross-sectional area of the magnetic bubble is comparable to the upstream ion inertial length of $\approx$100 km. Therefore, a considerably larger plasma sail would be required.

An obvious shortcoming of this model is the limited simulation domain that is computationally feasible with the three-dimensional hybrid code. A fully kinetic approach would be desirable for describing the self-consistent evolution of the magnetic bubble as well as improved boundary conditions for studying the steady-state configuration in the kinetic description. In addition, it will be critical to establish the scale length of the transition between a whistler-mediated and an MHD-mediated interaction in three dimensions for the plasma sail application. This TP concludes with a discussion of future plasma sail studies that utilize solar radiation pressure as an alternative source of momentum for improving the design of the plasma sail propulsion concept.

4.2 Future Plasma Sail Studies

An untapped resource in the plasma sail concept is the solar radiation flux (photons) which has several orders of magnitude higher force per unit area than the solar wind particle flux. For example, at 1 au the solar radiation pressure is 4.57×10^{-6} (Nm^{-2}) versus 6.7×10^{-10} (Nm^{-2}) solar wind dynamic pressure.[15] The inclusion of dust grains in a plasma bubble, which absorb or scatter solar radiation, may provide a significant improvement or even be enabling to plasma sail development.[16] Specifically, the scattering of solar photon flux can enable (1) enhanced mission performance as a result of increased thrust; i.e., increased payload and/or decreased time to destination, and (2) creation of an effective plasma sail of much smaller physical dimensions. As discussed in the previous sections, there is concern and disagreement regarding the size of a basic particle momentum transfer plasma sail required to produce a given thrust and plasma losses associated with larger systems. The latter capability will, therefore, be particularly useful if inflation and maintenance of the magnetic bubble is more difficult than predicted.

The radiation force on a 3-μm spherical silicon dioxide dust grain at 1 au is 3×10^{-16} N;[17] the charge on the grain is $\approx$1,500 e for the expected plasma environment.[16] Therefore a force of 1 N can be achieved with 3×10^{15} dust particles. It is assumed that (1) to minimize influence on the plasma, the total charge on the dust is only 0.5 percent of the charge of the confined plasma and is uniformly distributed; (2) the plasma density distribution falls off as $1/r^2$; and (3) the density of the plasma at the source is 10×10^{13} cm^{-3}.[1] Under these conditions the required size of the bubble is $\approx$1 km which is an order of magnitude smaller than the most optimistic estimates of a basic plasma sail. If the parameter $P = 695 T_d r_d (n_d/n) < 1$,[18] the dust particles can be considered isolated, which is the case for the parameters where the plasma temperature, T_d, is 0.3 eV, r_d is the grain size, and n_d/n is the ratio of the dust to plasma densities.

The confinement of dust within a plasma bubble is the most pressing question regarding the use of dust particles. Specifically, is the dust coupled strongly enough to the field lines to confine the grains against the radiation forces and thus provide momentum transfer? The Larmor radius of a 3-μm dust grain with 1 m/s velocity is 30 km near the solenoid and increases rapidly with radial distance. Magnetic confinement of the dust is, therefore, not possible. If the dust is to be confined, it must be through electrostatic forces. Several such mechanisms could potentially contribute to the confinement of charged dust grains. For example, motion of a charged dust grain out of the bubble will violate quasi-neutrality of the confined plasma and create an electrostatic force that opposes the motion.

APPENDIX A—MAGNETOHYDRODYNAMIC EQUATIONS AND NUMERICS

The ideal MHD equations describe the conservation of mass, momentum, and energy of a conducting fluid and the evolution of the magnetic field. These equations can be written in conservative form as follows:

$$\frac{\partial \rho}{\partial t} + \nabla \cdot (\rho \mathbf{u}) = 0 \tag{4}$$

$$\frac{\partial (\rho \mathbf{u})}{\partial t} + \nabla \cdot \left[\rho \mathbf{u}\mathbf{u} + \left(p + \frac{B^2}{2\mu_0} \right) I - \frac{\mathbf{B}\mathbf{B}}{\mu_0} \right] = 0 \tag{5}$$

$$\frac{\partial \mathbf{B}}{\partial t} + \nabla \cdot (\mathbf{u}\mathbf{B} - \mathbf{B}\mathbf{u}) = 0 \tag{6}$$

$$\frac{\partial \varepsilon}{\partial t} + \nabla \cdot \left[u \left(\varepsilon + p + \frac{B^2}{2\mu_0} \right) - \frac{(\mathbf{u} \cdot \mathbf{B})\mathbf{B}}{\mu_0} \right] = 0 \ , \tag{7}$$

where ρ is the plasma mass density, $\mathbf{u}$ is the plasma velocity, $\mathbf{B}$ is the magnetic field, p is the thermal pressure, and ε is the total energy density given by

$$\varepsilon = \frac{\rho u^2}{2} + \frac{p}{\gamma - 1} + \frac{B^2}{2\mu_0} \ . \tag{8}$$

This form of the MHD equations is solved using a modern high-resolution Godunov-type finite-volume method which is described in Powell et al.[19] The spatial discretization of the equations is performed on an adaptive unstructured Cartesian grid based on Octree technology.

Figure 8 shows a typical grid used in the MHD simulations presented in this TP. One can see grid refinement near the bow shock in front of the plasma sail and in the inner region near the central body. The simulations used ≈500,000 cells with sizes ranging from 50 km to 0.1 m (19 levels of refinement), allowing the different length scales of the problem to be resolved.

The outer boundary conditions in the simulation of the solar wind interaction with the plasma sail were super-fast inflow or outflow—all the parameters are simply prescribed at the outer edge of the simulation box. In the simulation of the plasma expansion into vacuum, the MHD variables from the computational domain were linearly extrapolated to the outer boundary, allowing the infinite space beyond the simulation area to be mimicked and possible effects of the boundary on the computed solution to be avoided. At the inner boundary the values of the MHD variables were prescribed in a layer of "ghost cells" just below the 10-m sphere in the same manner as described in, for example, Kabin et al.[7]
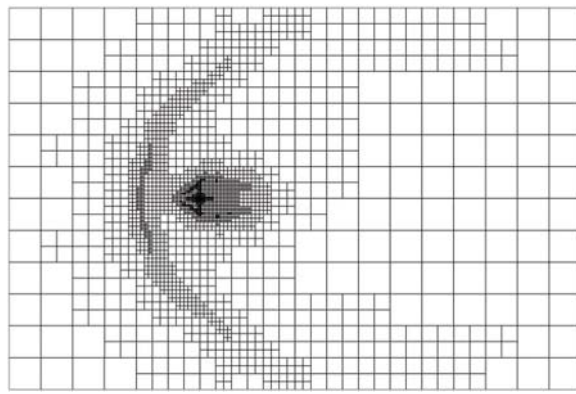
Figure 8. Grid used for a typical MHD simulation
of plasma sails.

APPENDIX B—HYBRID CODE EQUATIONS

The hybrid code was first proposed by Harned[20] and the particular algorithms for the code discussed in this TP were developed by Swift.[21,22] The code assumes quasi-neutrality and is nonradiative. The electric fields can be written explicitly from the electron momentum equation.

$$\mathbf{E} = -\mathbf{u}_e \times \mathbf{B} \ , \tag{9}$$

where $\mathbf{E}$ is the electric field in units of proton acceleration, $\mathbf{B}$ is the magnetic field in units of ion gyrofrequency, and $\mathbf{u}_e$ is the electron flow velocity. The electron flow speed is evaluated from Ampere's law,

$$\mathbf{u}_e = \mathbf{u}_i - \frac{\nabla \times \mathbf{B}}{\alpha n} \ , \tag{10}$$

where in mks units, $\alpha = \mu_0 e^2/m_i$, and where m_i is the ion mass, μ_0 is the permeability of free space and e is the electronic charge. The primary advantage for writing $\mathbf{B}$ in units of ion gyrofrequency is that α can be used to scale the simulation particle densities to their appropriate physical values.

Faraday's law is used to update the perturbation magnetic fields,

$$\frac{\partial \mathbf{B}}{\partial t} = -\nabla \times \mathbf{E} \tag{11}$$

or

$$\frac{\partial \mathbf{B}}{\partial t} = -\nabla \times \left[\left(\frac{\nabla \times \mathbf{B}}{\alpha n} - \mathbf{u}_i \right) \times \mathbf{B} \right] \ . \tag{12}$$

Note that $\mathbf{B} = \mathbf{B}_0 + \mathbf{B}_{dp} + \mathbf{B}_1$, where $\mathbf{B}_0$ is the ambient curl free interplanetary magnetic field, $\mathbf{B}_{dp}$ is the curl free dipole field, and $\mathbf{B}_1$ is the variable field. With the equation for the magnetic fields written in this form, it can be shown that the first term on the right hand side is responsible for the propagation of the whistler mode and the second term propagates the Alfvén modes.

The equation for the ion particle motion is

$$\frac{d\mathbf{v}}{dt} = \mathbf{E} + \mathbf{v} \times \mathbf{B} \ . \tag{13}$$

The code also provides an optional interface between the particle ion populations and a cold fluid description where the fluid ion motion is described by

$$\frac{\partial \mathbf{u}_f}{\partial t} = \mathbf{E}_f + \frac{n_p}{n}\mathbf{u}_f \times \mathbf{B} \ , \tag{14}$$

where

$$\mathbf{E}_f = -(\mathbf{u}_f \cdot \nabla)\mathbf{u}_f \ + \left(\frac{\nabla \times \mathbf{B}}{\alpha n} - \frac{n_p}{n}\mathbf{u}_p\right) \times \mathbf{B} \tag{15}$$

and

$$\mathbf{u}_i = \frac{n_p}{n}\mathbf{u}_p + \frac{n_f}{n}\mathbf{u}_f \ , \tag{16}$$

where the subscripts p and f refer to the ion particle and fluid components, respectively.

Momentum conservation for the hybrid code equations (no ion fluid component) is given by

$$\sum_{k=1}^{N_i} m_i \frac{dv_k}{dt} = \oint_s \tilde{T} \cdot da \ , \tag{17}$$

where the stress tensor is

$$T_{ij} \equiv \frac{m_i}{\alpha}\left(B_i B_j - \frac{1}{2}\delta_{ij}B^2\right) \tag{18}$$

The total change in momentum of a given volume element is therefore equal to the Maxwell stress on the boundaries. The electric field does not appear in the conservation expression due to the assumption of quasi-neutrality.

REFERENCES

1. Winglee, R.M.; Slough, J.; Ziemba, T.; and Goodson, A.: "Mini-Magnetospheric Plasma Propulsion: Tapping the energy of the solar wind for spacecraft propulsion," *J. Geophys. Res.*, Vol. 105(A9), p. 21,067, September 2000.

2. Saha, S.; Singh, N.; Craven, P.; Gallagher, D.; and Jones, J: "Development of 3D hybrid code and its application to M2P2" in *Proceedings of Space Technology and Applications International Forum 2002*, Albuquerque, NM, Vol. 608, p. 441, M.S. El-Genk, ed., American Institute of Physics, February 3–6, 2002.

3. Karimabadi, H.; and Omidi, N.: "Latest Advances in Hybrid Codes and Their Application to Global Magnetospheric Simulations," available online at http://ssc.igpp.ucla.edu/gem/tutorial/index.html, Geospace Environment Modeling Summer Workshop, Telluride, CO, June 24–28, 2002.

4. Winglee, R.M.; Ziemba, T.; Euripides, P.; and Slough, J.: "Magnetic inflation produced by the Mini-Magnetospheric Plasma Propulsion (M2P2) prototype," in *Proceedings of Space Technology and Applications International Forum 2002*, Albuquerque, NM, Vol. 608, p. 433, M.S. El-Genk, ed., American Institute of Physics, February 3–6, 2002.

5. Linde, T.J.; Gombosi, T.I.; Roe, P.L; Powell, K.G.; and DeZeeuw, D.L.: "The Heliosphere in the magnetized local interstellar medium: results of a 3D MHD simulation," *J. Geophys. Res.*, 103(A2), p. 1,889, February 1998.

6. Kabin, K.; Gombosi, T.I.; DeZeeuw, D.L.; Powell, K.G.; Israelevich, P.L.: "Interaction of the Saturnian magnetosphere with Titan: Results of a 3D MHD simulation," *J. Geophys. Res.*, 104(A2), p. 2,451, February 1999.

7. Kabin, K.; Combi, M.R.; Gombosi, T.I.; Nagy, A.F.; DeZeeuw, D.L.; Powell, K.G.: "On Europa's magnetospheric interaction: A MHD simulation of the E4 flyby," *J. Geophys. Res*, 104(A9), p. 19,983, September 1999.

8. Kabin, K.; Hansen, K.C.; Gombosi, T.I.; Combi, M.R.; Linde, T.J.; DeZeeuw, D.L.; Groth, C.P.T.; Powell, K.G.; and Nagy, A.F.: "Global MHD simulations of space plasma environments: Heliosphere, comets, magnetospheres of planets and satellites," *Astrophysics and Space Science*, 274(1/2), p. 407, 2000.

9. Nagy, A.F.; Liu, Y.; Hansen, K.C.; Kabin, K.; Gombosi, T.I.; Combi, M.R.; DeZeeuw, D.L.; Powell, K.G.; Kliore, A.J.: "The interaction between the magnetosphere of Saturn and Titan's ionosphere," *J. Geophys. Res.*, 106(A4), p. 6,151, April 2001.

10. Sisco, G.L.: "Solar System Magnetohydrodynamic," *Solar-Terrestrial Physics*, D. Reider Publishing Co., Boston, MA, p. 11, 1983.

11. Delamere, P.A.; Swift, D.W.; Stenbaek-Nielsen, H.C.: "A three-dimensional hybrid code simulation of the December 1984 solar wind AMPTE release," *Geophys. Res. Let.*, Vol. 26, p. 2,837, 1999.

12. Delamere, P.A.; Swift, D.W.; Stenbaek-Nielsen, H.C.; and Otto, A.: "Momentum transfer in the CRRES plasma injection experiments: The role of parallel electric fields," *Physics of Plasmas*, Vol. 7, p. 3,771, 2000.

13. Wang, Z.; and Kivelson, M.G.: "Asteroid interaction with solar wind," *J. Geophys. Res.*, 101(A11), p. 24,479, November 1996.

14. Kuethe, A.M.; and Chow, C.-Y.: *Foundations of Aerodynamics: Bases of Aerodynamic Design, Third Edition*, 527 pp., John Wiley & Sons, New York, 1976.

15. Parks, G.: *Physics of Space Plasmas: An Introduction, First Edition*, 538 pp., Perseus Book Group, 1991.

16. Sheldon, R.; Thomas, E., Jr.; Abbas, M.; Gallagher, D.; Adrian M.; and Craven, P.: "Dynamic and optical characterization of dusty plasmas for use as solar sails," in *Proceedings of Space Technology and Applications International Forum 2002*, Albuquerque, NM, Vol. 608, p. 425, M.S. El-Genk, ed., American Institute of Physics, February 3–6, 2002.

17. Abbas, M.M.; Craven, P.D.; Spann, J.F.; et al.: "Radiation pressure measurement on micron size individual dust grains," *J. Geophys. Res.*, Vol. 108(A6), p. 1,229, June 2003.

18. Havnes, O.; Goertz, C.K.; Morfill, G.E.; Grun, E.; and Ip, W.: "Dust charges, cloud potential, and instabilities in a dust cloud embedded in a plasma," *J. Geophys. Res.*, Vol. 92(A3), p. 2,281, 1987.

19. Powell, K.G.; Roe, P.L.; Linde, T.J.; Gombosi, T.I.; and DeZeeuw D.L.: "A solution-adaptive upwind scheme for ideal magnetohydrodynamics," *J. Comput. Phys.*, Vol. 154(2), p. 284, September 1999.

20. Harned, D.S.: "Quasineutral hybrid simulation of macroscopic plasma phenomena," *J. Comput. Phys.*, Vol. 47, p. 452, 1982.

21. Swift, D.W.: "Use of a hybrid code to model the Earth's magnetosphere," *Geophys. Res. Let.*, Vol. 22, p. 311, 1995.

22. Swift, D.W.: "Use of a hybrid code for global-scale plasma simulation," *J. Comput. Phys.*, Vol. 126(1), p. 109, November 1996.

REPORT DOCUMENTATION PAGE

Form Approved
OMB No. 0704-0188

1. AGENCY USE ONLY *(Leave Blank)*	2. REPORT DATE April 2004	3. REPORT TYPE AND DATES COVERED Technical Publication

4. TITLE AND SUBTITLE

Plasma Sail Concept Fundamentals

5. FUNDING NUMBERS

6. AUTHORS

G.V. Khazanov, P. Delamere,* K. Kabin,** and T.J. Linde***

7. PERFORMING ORGANIZATION NAMES(S) AND ADDRESS(ES)

George C. Marshall Space Flight Center
Marshall Space Flight Center, AL 35812

8. PERFORMING ORGANIZATION REPORT NUMBER

M–1103

9. SPONSORING/MONITORING AGENCY NAME(S) AND ADDRESS(ES)

National Aeronautics and Space Administration
Washington, DC 20546–0001

10. SPONSORING/MONITORING AGENCY REPORT NUMBER

NASA/TP—2004–213143

11. SUPPLEMENTARY NOTES
Prepared by the Space Science Department, Science Directorate
*Laboratory for Atmospheric and Space Physics, University of Colorado, Boulder, CO **Department of Physics, University of Alberta, Alberta, Canada ***The University of Chicago, Chicago, IL

12a. DISTRIBUTION/AVAILABILITY STATEMENT

Unclassified-Unlimited
Subject Category 20
Available: NASA CASI (301)621–0390

12b. DISTRIBUTION CODE

13. ABSTRACT *(Maximum 200 words)*

The mini-magnetospheric plasma propulsion (M2P2) device, originaly proposed by Winglee et al., predicts that a 15-km standoff distance (or 20-km cross-sectional dimension) of the magnetic bubble will provide for sufficient momentum transfer from the solar wind to accelerate a spacecraft to unprecedented speeds of 50–80 km/s after an acceleration period of $\approx$3 mo. Such velocities will enable travel out of the solar system in period of $\approx$7 yr—almost an order of magnitude improvement over present chemical-based propulsion systems. However, for the parameters of the simulation of Winglee et al., a fluid model for the interaction of M2P2 with the solar wind is not valid. It is assumed in the magnetohydrodynamic (MHD) fluid model, normally applied to planetary magnetospheres, that the characteristic scale size is much greater than the Larmor radius and ion skin depth of the solar wind. In the case of M2P2, the size of the magnetic bubble is actually less than or comparable to the scale of these characteristic parameters. Therefore, a kinetic approach, which addresses the small-scale physical mechanisms, must be used. A two-component approach to determining a preliminary estimate of the momentum transfer to the plasma sail has been adopted. The first component is a self-consistent MHD simulation of the small-scale expansion phase of the magnetic bubble. The fluid treatment is valid to roughly 5 km from the source and the steady-state MHD solution at the 5 km boundary was then used as initial conditions for the hybrid simulation. The hybrid simulations showed that the forces delivered to the innermost regions of the plasma sail are considerably ($\approx$10 times) smaller than the MHD counterpart, are dominated by the magnetic field pressure gradient, and are directed primarily in the transverse direction.

14. SUBJECT TERMS
plasma sail, plasma propulsion, solar wind, magnetohydrodynamic model, kinetic model

15. NUMBER OF PAGES
32

16. PRICE CODE

17. SECURITY CLASSIFICATION OF REPORT Unclassified	18. SECURITY CLASSIFICATION OF THIS PAGE Unclassified	19. SECURITY CLASSIFICATION OF ABSTRACT Unclassified	20. LIMITATION OF ABSTRACT Unlimited